INFECTION AND IMMUNITY, Aug. 2002, p. 4353–4361 Vol. 70, No. 8
0019-9567/02/$04.00+0 DOI: 10.1128/IAI.70.8.4353–4361.2002

Clostridium septicum Alpha-Toxin Is Active against the Parasitic Protozoan *Toxoplasma gondii* and Targets Members of the SAG Family of Glycosylphosphatidylinositol-Anchored Surface Proteins

Michael J. Wichroski,[1] Jody A. Melton,[2] Carolyn G. Donahue,[1] Rodney K. Tweten,[2] and Gary E. Ward[1]*

Department of Microbiology and Molecular Genetics, University of Vermont, Burlington, Vermont 05405,[1] and Department of Microbiology and Immunology, University of Oklahoma Health Sciences Center, Oklahoma City, Oklahoma 73190[2]

Received 22 January 2002/Returned for modification 5 March 2002/Accepted 8 May 2002

As is the case with many other protozoan parasites, glycosylphosphatidylinositol (GPI)-anchored proteins dominate the surface of *Toxoplasma gondii* tachyzoites. The mechanisms by which *T. gondii* GPI-anchored proteins are synthesized and transported through the unusual triple-membrane structure of the parasite pellicle to the plasma membrane remain largely unknown. As a first step in developing tools to study these processes, we show here that *Clostridium septicum* alpha-toxin, a pore-forming toxin that targets GPI-anchored protein receptors on the surface of mammalian cells, is active against *T. gondii* tachyzoites (50% effective concentration, 0.2 nM). Ultrastructural studies reveal that a tight physical connection between the plasma membrane and the underlying membranes of the inner membrane complex is locally disrupted by toxin treatment, resulting in a massive outward extension of the plasma membrane and ultimately lysis of the parasite. Toxin treatment also causes swelling of the parasite endoplasmic reticulum, providing the first direct evidence that alpha-toxin is a vacuolating toxin. Alpha-toxin binds to several parasite GPI-anchored proteins, including surface antigen 3 (SAG3) and SAG1. Interestingly, differences in the toxin-binding profiles between the virulent RH and avirulent P strain were observed. Alpha-toxin may prove to be a powerful experimental tool for molecular genetic analysis of GPI anchor biosynthesis and GPI-anchored protein trafficking in *T. gondii* and other susceptible protozoa.

Toxoplasma gondii is parasitic protozoan that infects a broad range of warm-blooded hosts, including humans. It is a member of the phylum Apicomplexa, which also includes *Plasmodium*, the causative agent of malaria. The disease caused by *T. gondii*, toxoplasmosis, is of considerable medical importance, because it can lead to birth defects and death in the congenitally infected fetus and can have devastating consequences in the immunocompromised host. *T. gondii* is an obligate intracellular parasite, and the highly invasive asexual stage, the tachyzoite, exhibits an extraordinary promiscuity in the range of mammalian host cells it is capable of infecting (47).

As is the case with many other parasitic protozoa (18, 19, 31, 32), glycosylphosphatidylinositol (GPI)-anchored proteins dominate the plasma membrane of the *T. gondii* tachyzoite. The abundant GPI-anchored surface antigens (SAGs) of *T. gondii* are immunogenic and share common primary sequence features that suggest a conserved overall topology (6, 9, 11, 27–29). The SAGs are likely to be densely packed on the parasite surface; SAG1 alone constitutes 3 to 5% of total cell protein (25), equivalent to 1.5×10^6 to 2.5×10^6 copies/cell. Free GPIs have also been identified on the surface of *T. gondii* tachyzoites (41; B. Striepen, S. Tomavo, J. F. Dubremetz, and R. T. Schwarz, abstract from 642nd Meet. Biochem. Soc. [United Kingdom] 1992, Biochem. Soc. Trans. **20:**296S, 1992), although their abundance relative to other well-studied parasites remains unknown (18, 19, 31, 32).

Our current understanding of GPIs in *T. gondii* has been limited to biochemical studies describing the mature protein-bound anchor and intermediates along the GPI anchor biosynthetic pathway (40–44, 49; Striepen et al., Biochem. Soc. Trans. **20:**296S, 1992; S. Tomavo, J. F. Dubremetz, and R. T. Schwarz, abstract from 641st Meet. Biochem. Soc. [United Kingdom] 1991, Biochem. Soc. Trans. **20:**166S, 1992). We are interested in how GPIs and GPI-anchored proteins are synthesized and trafficked to the parasite surface through the three tightly apposed lipid bilayers that constitute the parasite pellicle. As a first step in developing a genetic selection strategy for mutants in GPI anchor biosynthesis and transport, we investigated whether *Clostridium septicum* alpha-toxin (AT) is active against *T. gondii* tachyzoites. AT is a pore-forming toxin and a major virulence factor associated with a frequently fatal, nontraumatic gas gangrene (39). It is secreted as a soluble protoxin that can be activated through proteolysis by cell surface proteases, including furin (21). Activation leads to oligomerization of monomeric subunits and ultimately to insertion of this complex into the plasma membrane of mammalian cells, generating a pore approximately 1.3 to 1.6 nm in diameter (2, 4). Pore formation by AT induces selective membrane permeabilization of erythrocytes to small ions, followed by hemolysis (4, 38).

* Corresponding author. Mailing address: Department of Microbiology and Molecular Genetics, University of Vermont, Burlington, VT 05405. Phone: (802) 656-4868. Fax: (802) 656-8749. E-mail: gward@zoo.uvm.edu.

The subcellular effects of AT pore formation on nucleated mammalian cells have not been reported. The binding of AT to GPI-anchored proteins in toxin overlays, the inability of the toxin to bind to the surface of GPI-deficient mammalian cells, and the resistance of these cells to the cytolytic action of the toxin all strongly suggest that AT exclusively uses cell surface GPI-anchored proteins as receptors (22). AT demonstrates selectivity for certain GPI-anchored proteins over others, indicating that specific modifications to the GPI moiety and/or protein determinants influence receptor recognition (22).

In this report, we show that AT is active against *T. gondii* tachyzoites at concentrations similar to those that are toxic to mammalian cells. Neither the high density of GPI-anchored proteins on the parasite surface nor the triple-bilayer structure of the pellicle constitutes a barrier against the cytolytic activity of AT. This is the first demonstration that AT is active against nonmetazoan cells and provides further evidence that the critical determinant for AT pore formation is the presence of GPI-anchored protein targets. We show that AT is a vacuolating toxin, and we use the toxin to provide direct evidence that the plasma membrane of the parasite is physically tethered to the underlying inner membrane complex. Finally, AT appears to bind differentially to the SAG proteins of virulent and avirulent strains of *T. gondii*. These studies suggest that AT will be a valuable tool for studying the biosynthesis, transport, and structure of GPI-anchored proteins in *T. gondii* and other susceptible protozoa.

MATERIALS AND METHODS

Parasite culture. The following *T. gondii* tachyzoite strains were used: RH(EP)Δ*HXGPRT* (34, 37) (used to facilitate future molecular genetic manipulation of the parasite and referred to hereafter simply as RH), RHΔ*SAG3* (17) and the parental clone from which this mutant was derived (designated here as RH[ST]; both generous gifts from Stanislas Tomavo), and P(LK)*sag1* and its parental P(LK) strain (25) (both generously provided by L. Kasper). Parasites were cultured in human foreskin fibroblasts (HFFs) (CRL 1634; American Type Culture Collection, Rockville, Md.) as previously described (37). For all experiments, tachyzoites were harvested from freshly lysed HFF monolayers and filtered through 3-μm-pore-diameter Nuclepore syringe filters (Whatman, Clifton, N.J.) to remove host cell debris prior to use. All chemicals were purchased from (Sigma, St. Louis, Mo.) unless otherwise indicated.

Activation of AT. Prior to use, purified recombinant protoxin (38) was activated by incubation with tosylsulfonyl phenylalanyl choloromethyl ketone (TPCK)-treated trypsin at a 1:3,500 (wt/wt) trypsin/toxin ratio for 30 min at 37°C in activation buffer (0.5 M NaCl, 10 mM morpholineethanesulfonic acid [MES; pH 6.5], 1 mM EDTA, 10% [vol/vol] glycerol). Following activation, the trypsin was inactivated with 3 μg of phenylmethylsulfonyl fluoride per μg of AT. In experiments in which prolonged cell culture was required, activated AT was dissolved in culture medium and filter sterilized through 0.2-μm-pore-diameter syringe filters (PALL Company, Ann Arbor, Mich.).

AT cytotoxicity assay. The effect of AT on parasite viability was determined by plaque assay (35). Tachyzoites (5×10^6) were incubated in 96-well plates for 1 h (37°C, humidified incubator) in 200 μl of parasite culture medium containing various concentrations of AT. After treatment, tachyzoites were plated onto monolayers of HFFs in T-25 culture flasks at a range of dilutions that allowed for the counting of individual plaques. The cultures were then incubated undisturbed for 6 to 9 days, and plaques were scored visually. Results are expressed as a percentage of the number of plaques formed by control (untreated) parasites at the equivalent parasite dilution.

Immunofluorescence microscopy. Freshly harvested tachyzoites were washed twice with phosphate-buffered saline (PBS; pH 7.4) (137 mM NaCl, 2.7 mM KCl, 10 mM Na_2HPO_4, 2 mM KH_2PO_4) and attached to coverglasses with Cell-Tak (Collaborative Biomedical Products, Bedford, Mass.) as previously described (45). The samples were washed three times in PBS and fixed on ice for 30 min in PBS containing 2.5% (vol/vol) paraformaldehyde and 0.025% (vol/vol) glutaraldehyde (Electron Microscopy Sciences, Washington, Pa.). Fixed samples were incubated (10 min, on ice) in PBS containing 0.5% (wt/vol) bovine serum albumin (PBS/BSA) ± 0.1% (vol/vol) Triton X-100, followed by a 30-min incubation on ice with fluorescently conjugated monoclonal antibodies (MAbs) in PBS/BSA ± 0.1% Triton X-100. The MAbs used were MAb G11-9 against SAG1 (Argene, Inc., Varihes, France), MAb 17.9 against GRA6 (10), and MAb 45.15 (K. L. Carey and G.E.W., unpublished data) against the inner membrane complex (IMC) protein IMC1 (30). MAbs were directly conjugated to either Alexa 488 or Alexa 546 according to the manufacturer's instructions (Molecular Probes, Eugene, Oreg.). The coverglasses were washed three times in PBS, mounted onto slides, and observed with a Nikon TE300 inverted microscope equipped with epifluorescence illumination and differential interference contrast optics with a PlanApo ×100 oil immersion objective. Digital images were captured with a SpotRT monochrome camera driven by Spot v.3.01 (AppleEvent) software (Diagnostic Instruments, Sterling Heights, Mich.) and processed with Adobe Photoshop 6.0 (Adobe Systems, Mountain View, Calif.).

Electron microscopy. Freshly harvested tachyzoites were incubated in parasite culture medium with 10 nM AT for 30, 60, and 240 min at 37°C. Treated tachyzoites were washed twice in PBS (pH 7.4) and fixed in PBS containing 3% (vol/vol) formaldehyde and 0.1% (vol/vol) glutaraldehyde for 2 h at 22°C. Cells were washed two additional times in PBS and resuspended in PBS containing 2% (wt/vol) agarose at 37°C. The agarose cell pellet was allowed to harden on ice and was cut into 1-mm^2 blocks. The specimens were fixed in Karnovsky's reagent for 12 h at 4°C, and fresh Karnovsky's reagent was used for washing (15 min). Specimens were washed three times in Millonig's buffer (0.1 M sodium phosphate buffer [pH 7.4], 0.43 M NaCl) and fixed in 1% (wt/vol) osmium tetroxide (Electron Microscopy Sciences) for 30 min at 4°C. The cells were then sequentially dehydrated in increasing concentrations of ethanol and embedded in Spurr's resin (Electron Microscopy Sciences) as per the manufacturer's instructions. Thin sections were deposited on copper grids (Electron Microscopy Sciences), contrasted with 2% (wt/vol) uranyl acetate (Fluka, Milwaukee, Wis.) in 50% (vol/vol) ethanol and lead citrate solution, and observed with a Jeol 1210 transmission electron microscope.

Triton X-114 phase partitioning and PI-PLC cleavage of GPI anchors. Freshly harvested tachyzoites were lysed in extraction buffer made up of 10 mM Tris (pH 7.4), 150 mM NaCl, 0.5% (vol/vol), and precondensed (7) Triton X-114 (Pierce, Rockford, Ill.) containing protease inhibitors [5 μg of 4-(2-aminoethyl)benzenesulfonyl fluoride (AEBSF) per ml, 2 μg of aprotinin per ml, 2 μg of leupeptin per ml, 16 μg of benzamidine per ml, 5 μg of pepstatin per ml] for 90 min on ice. The samples were cleared twice by centrifugation (14,000 × *g*, 4°C, 5 min), incubated for 5 min at 37°C, and separated into detergent and aqueous phases as previously described (10). Cleavage of GPI anchors was performed prior to phase partitioning by incubating cleared extracts with 3 U of *Bacillus cereus* phosphatidylinositol-specific phospholipase C (PI-PLC) per ml (Molecular Probes) for 60 min at 37°C.

SDS-PAGE, silver stain, and Western blotting. Protein samples were boiled in nonreducing or reducing (5% [vol/vol] β-mercaptoethanol) sodium dodecyl sulfate-polyacrylamide gel electrophoresis (SDS-PAGE) sample buffer, resolved by SDS-PAGE, and either subjected to silver staining (10) or directly transferred to nitrocellulose (Schleicher & Schuell, Keene, N.H.) for Western blotting with a Semi-Dry Electroblotter (Integrated Separation Systems, Natick, Mass.). For the silver-stained gel/toxin overlays shown in Fig. 5, protein recovered from $4 \times 10^6/2 \times 10^6$ parasite equivalents was loaded for the total and detergent-phase (minus PI-PLC) samples; $8 \times 10^6/4 \times 10^6$ parasite equivalents was loaded for all other samples to make up for protein loss during phase partitioning. For the samples shown in Fig. 6, loads were normalized to protein content (2 μg per lane for silver staining and 1 μg per lane for Western blots) using the Pierce Micro BCA (bicinchoninic acid) kit.

Following transfer, blots were blocked overnight in 5% (wt/vol) nonfat dry milk in TBS-T (20 mM Tris [pH 7.4], 150 mM NaCl, 0.1% Tween 20) and washed three times for 10 min each in TBS-T before and after the addition of toxin or antibody. All toxins and antibodies were also diluted in TBS-T. For the toxin overlays, blots were incubated with 20 nM pro-AT or 20 nM pro-aerolysin (a generous gift of J. Thomas Buckley) and probed with either an anti-AT rabbit polyclonal antibody (2) or an anti-aerolysin mouse MAb (a generous gift of J. Thomas Buckley). The SAG1 blots were probed with an anti-SAG1 mouse MAb (Argene; 1/2,000 [vol/vol]), and the SAG3 blots were probed with an anti-SAG3 mouse MAb (a generous gift of Jean-Francois Dubremetz; 1/1,000 [vol/vol]). Blots were incubated for 45 min with secondary antibodies directly conjugated to horseradish peroxidase (1/2,000 [vol/vol]) and developed by enhanced chemiluminescence (Amersham Life Sciences, Arlington Heights, Ill.). For probing blots sequentially with different antibodies, blots were washed in PBS twice for 5 min each time and then stripped with 4% (vol/vol) trichloroacetic

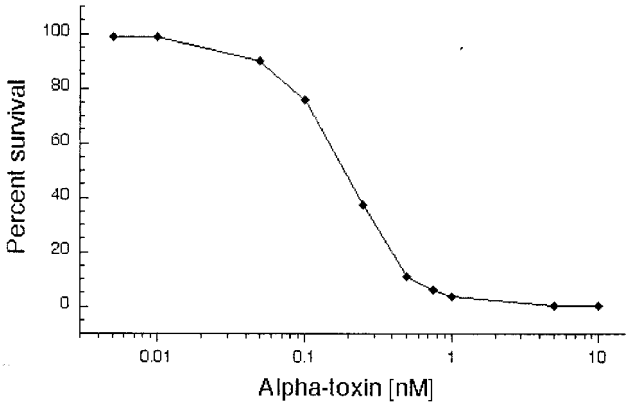

FIG. 1. Effects of AT treatment on the viability of *T. gondii* (RH) tachyzoites. Tachyzoites were incubated with various concentrations of AT for 60 min at 37°C. Viability was determined by plaque assay and is presented as the percentage of the number of plaques formed by control (untreated) parasites.

acid in PBS twice for 10 min each time. The blots were further washed twice in PBS and blocked again before use.

RESULTS

Sensitivity of *T. gondii* tachyzoites to AT. AT cytotoxicity was assayed by determining the viability of *T. gondii* tachyzoites after a 60-min incubation with various concentrations of activated AT (Fig. 1). Tachyzoites were sensitive to low concentrations of AT (50% effective concentration [EC_{50}] of 9 ng/ml [0.2 nM]; EC_{99} of 135 ng/ml [3 nM]). The majority of cell death occurred within 60 min, and there was no significant increase up to 240 min (data not shown). Incubation of parasites with the protoxin yielded a similar dose-response curve, suggesting that a parasite-derived protease may activate the toxin; however, we could not rule out the possibility of contaminating host cell proteases (data not shown).

AT induces vacuolation and the formation of massive membrane blebs in otherwise intact tachyzoites. Tachyzoites were incubated with 10 nM AT for 30, 60, and 240 min and examined by light microscopy (Fig. 2). After 30 min of AT treatment, tachyzoites had become swollen, losing their typical crescent shape. A distinct intracellular vacuole often developed (Fig. 2, arrowhead), and small membrane protrusions were observed. By 60 min of incubation, a membrane bleb appeared that ultimately became massive relative to the tachyzoite by the end of the time course (Fig. 2, arrows). While the plaque assays clearly demonstrated that these grossly distorted parasites were not viable, many were nonetheless able to de-esterify calcein AM ester and to exclude ethidium homodimer, suggesting that their plasma membranes remained intact (data not shown). *T. gondii* is an obligate intracellular parasite that depends on regulated motility and coordinated secretion from a polarized set of secretory organelles (the micronemes,

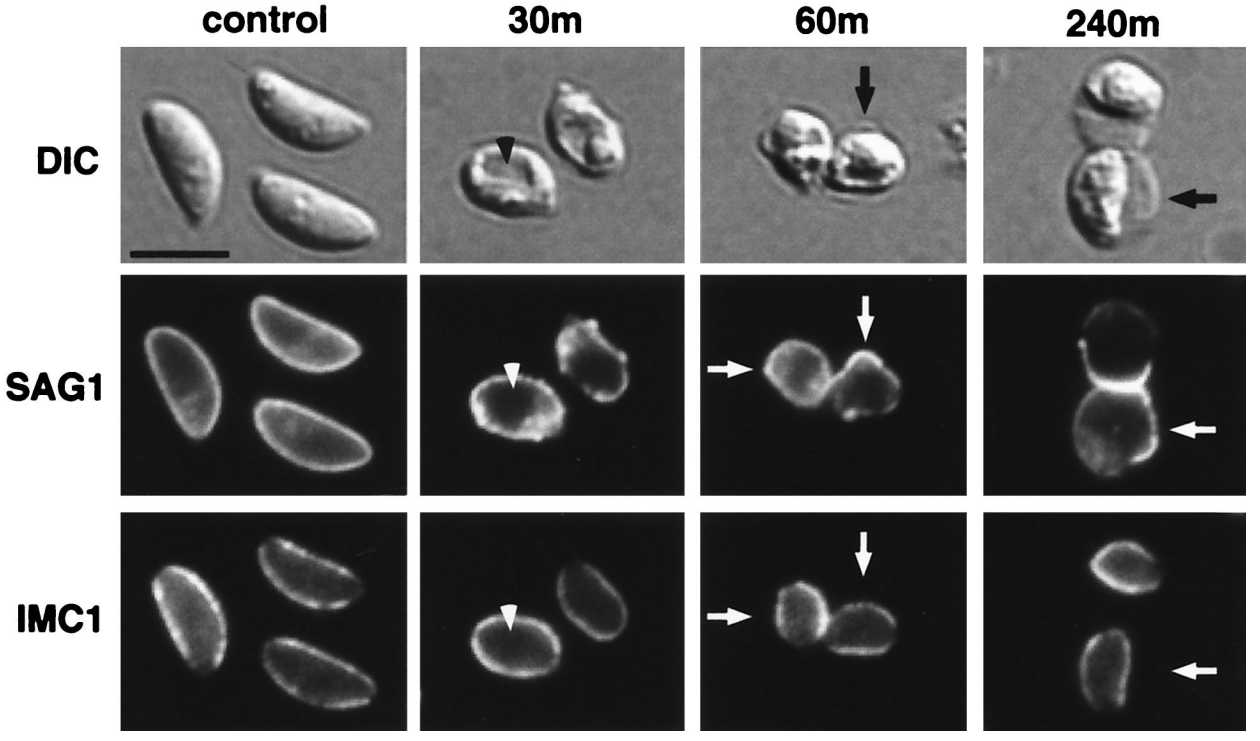

FIG. 2. Characterization of AT-treated tachyzoites by immunofluorescence and differential interference contrast (DIC) microscopy. Tachyzoites were incubated with 10 nM AT for 30, 60, or 240 min. Fixed and permeabilized parasites were then dual labeled with fluorescently conjugated MAbs against the GPI-anchored surface protein SAG1 and the inner membrane complex protein IMC1. After 30 min of AT treatment, a distinct vacuole was observed in most cells (arrowhead), and membrane protrusions were apparent. Between 60 and 240 min, massive membrane blebs appeared (arrows). The membrane blebs exhibited peripheral staining with the anti-SAG1 antibody, but not with the antibody against the IMC antigen; the distribution of the IMC antigen appeared unaffected by AT treatment. Scale bar, 5 μm.

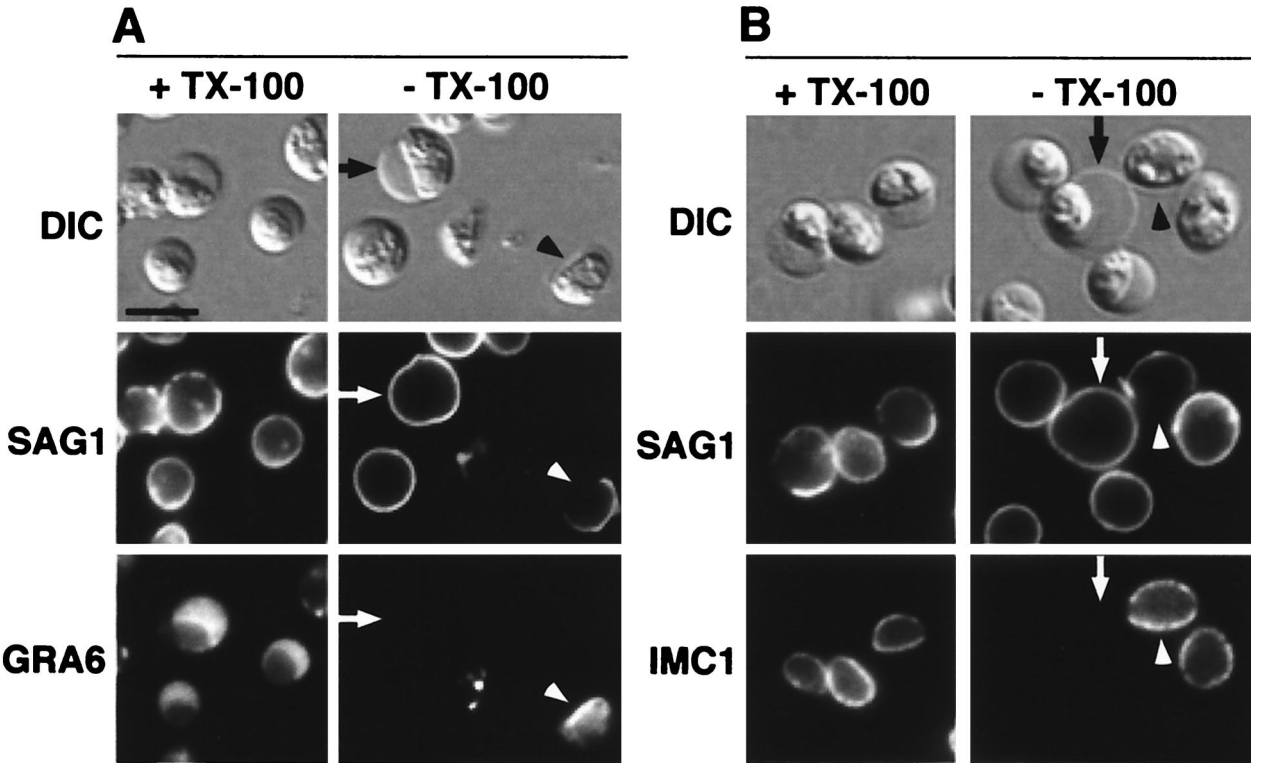

FIG. 3. Immunofluorescence analysis of fixed and permeabilized versus nonpermeabilized AT-treated tachyzoites. Tachyzoites were treated for 240 min with 10 nM AT, fixed, and processed for immunofluorescence with (+TX-100) or without (−TX-100) detergent (Triton X-100) permeabilization. Parasites were dual labeled with MAbs against the surface protein SAG1 and the dense granule protein GRA6 (A) or SAG1 and IMC1 (B). Arrows indicate toxin-induced membrane blebs, and arrowheads point to sites at which plasma membrane had ruptured. Scale bar, 5 μm.

rhoptries, and dense granules) for successful host cell invasion (reviewed in reference 5). Thus, it is not surprising that these morphologically disrupted parasites were functionally dead, even though their plasma membrane apparently remained intact.

The pellicle of the tachyzoite is a trimembranous structure consisting of the two membranes of the IMC tightly apposed to the plasma membrane (reviewed in reference 5). It was unclear whether the AT-induced membrane bleb was the result of swelling of the entire pellicle or just of the plasma membrane. We addressed this question by dual immunofluorescence with MAbs against the plasma membrane GPI-anchored protein SAG1 and IMC1. The membrane bleb exhibited peripheral SAG1 staining throughout the time course of AT treatment (Fig. 2, arrows). In contrast, the IMC remained restricted to its original distribution at all time points (Fig. 2, arrows), indicating that the bleb resulted from swelling of the plasma membrane and not of the entire pellicle.

The structural integrity of the membrane bleb after 240 min of toxin treatment was examined with MAbs against markers of the plasma membrane, IMC, and dense granules (GRA6). Tachyzoites were fixed and either permeabilized with Triton X-100 or processed without permeabilization (Fig. 3). Both permeabilized and unpermeabilized cells exhibited peripheral SAG1 staining (Fig. 3A, arrows), while the MAbs against intracellular targets were excluded from unpermeabilized cells, except where the plasma membrane bleb had ruptured (Fig. 3A and B, arrowheads). In these instances, a distinct gap in SAG1 staining was observed, showing that rupture of the plasma membrane bleb did not result in a complete dissociation of the remaining plasma membrane from the cell (described below). Ruptured cells no longer excluded MAbs against antigens of the dense granules (Fig. 3A) or the IMC (Fig. 3B). Furthermore, GRA6 showed a marked concentration near the IMC at the plasma membrane bleb site and localized diffusely within the lumen of the membrane bleb (Fig. 3A, arrowhead), indicating either lysis or secretion of the dense granules.

Electron microscopy of AT-treated tachyzoites. We next examined the effects of AT on tachyzoite ultrastructure by transmission electron microscopy (Fig. 4). After 30 min of AT treatment, tachyzoites lost their typical crescent shape and appeared swollen. Distinct cytoplasmic vacuoles were apparent, but the nucleus, dense granules, and rhoptries remained identifiable. By 60 min, the majority of tachyzoites exhibited a large perinuclear vacuole that, in most cases (Fig. 4A), was observed to be continuous with the outer nuclear membrane, a subcompartment of the endoplasmic reticulum (23). No intracellular organelles were identifiable, with the exception of the nucleus, which appeared intact. The majority of tachyzoites also exhibited an outward membrane bleb that expanded to massive proportions by the end of the 240-min time course and clearly contained cytoplasmic contents (consistent with the immunofluorescence data showing GRA6 within the lumen of the

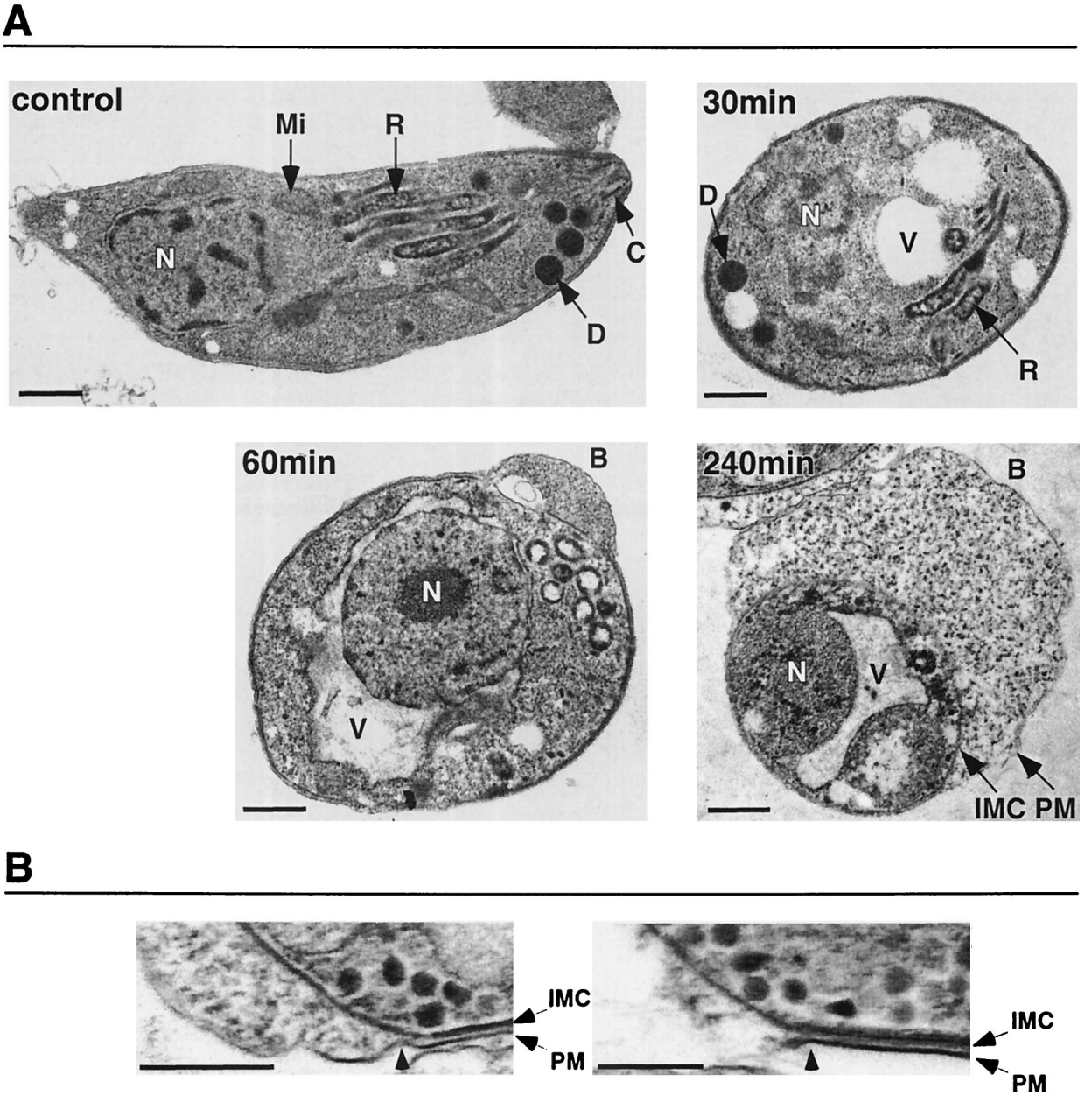

FIG. 4. Ultrastructural effects of AT. (A) Tachyzoites were incubated with 10 nM AT for 0, 30, 60, and 240 min and examined by transmission electron microscopy. Labels indicate the nucleus (N), mitochondria (Mi), rhoptry (R), dense granule (D), conoid (C), plasma membrane (PM), IMC, vacuole (V), and AT-induced plasma membrane bleb (B). Scale bars, 400 nm. (B) Higher-magnification micrographs of an intact bleb (left panel; arrowhead indicates the site of separation between the PM and IMC) and a ruptured bleb (right panel; arrowhead indicates the site of PM rupture.) Scale bars, 400 nm.

bleb) (Fig. 3A). The association between the IMC and plasma membrane appeared to be uncompromised, except where blebbing had occurred, as demonstrated by the tight association of the membranes near the bleb site (Fig. 4B, left panel). The segments of the plasma membrane that persisted after bleb rupture also appeared to maintain their tight association with the IMC (Fig. 4B, right panel).

AT recognizes parasite GPI-anchored proteins. In toxin overlays of total tachyzoite lysates (Fig. 5A), AT reproducibly bound to proteins of 54, 38, and 32 kDa and multiple lower-molecular-mass proteins (~18 to 25 kDa). To determine if these proteins were membrane associated, lysates were phase partitioned in Triton X-114; all but the 54-kDa protein were recovered in the detergent phase. The detergent-phase proteins partitioned into the aqueous phase after PI-PLC treatment, as would be expected for GPI-anchored proteins. The corresponding silver-stained gel shows that phase partitioning and PI-PLC treatment were both efficient and complete, as evidenced by the behavior of SAG1, the major silver-stained protein in the detergent phase (Fig. 5A, asterisk). This was

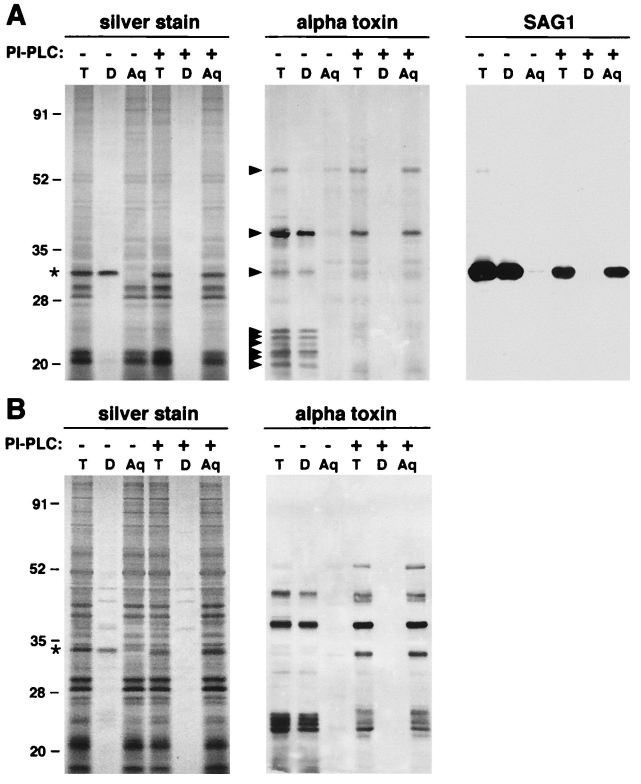

FIG. 5. AT binds to GPI-anchored parasite proteins. A Triton X-114 extract of tachyzoites (T) was incubated with or without PI-PLC and phase partitioned into detergent (D) and aqueous (Aq) phases. The fractions were analyzed by SDS-PAGE under nonreducing (A) or reducing (B) conditions. The gels were either silver stained or transferred to nitrocellulose for toxin overlay or SAG1 Western blotting. Under nonreducing conditions, AT binds to proteins with approximate molecular masses of 54, 38, and 32 kDa and multiple lower-molecular-mass (~18 to 25 kDa) proteins (arrowheads). All of these toxin-binding proteins (with the exception of the 54-kDa protein) partition into the detergent phase in the absence of PI-PLC treatment and into the aqueous phase after incubation with PI-PLC. AT binds significantly less protein after delipidation, a property that can be reversed by running the samples under reducing conditions. The major silver-stained protein in the detergent phase (asterisk) corresponds to SAG1. A SAG1 Western blot could not be run under reducing conditions, because the MAb does not recognize reduced protein. Numbers on the left indicate molecular mass in kilodaltons.

confirmed by Western blotting with a MAb against SAG1 (Fig. 5A). The 32-kDa AT-binding protein comigrates with SAG1, as shown by silver staining and Western blotting; further experiments (described below) have confirmed its identity as SAG1.

Comparison of the AT overlays before and after PI-PLC treatment suggested that AT binding was adversely affected by delipidation (Fig. 5A). This was unexpected, because the toxin is thought to recognize determinants within the glycan portion of the GPI anchor, which remains with the protein after PI-PLC cleavage (22). When the identical samples were electrophoresed under reducing conditions, the decrease in AT binding after delipidation was no longer observed (Fig. 5B). Once again, all of the AT-binding proteins (with the exception of the 54-kDa protein) exhibited phase-partitioning behavior consistent with GPI-anchored proteins. The profiles of AT-binding proteins were different on reduced and nonreduced gels (compare AT results in Fig. 5A and B). This likely reflects, at least in part, the previous observation that many SAG proteins migrate differently under reducing and nonreducing conditions (12, 27, 29) (note also the different mobilities of SAG1 in Fig. 5A and B). The reactivity of the SAG1 MAb used in these studies was diminished after PI-PLC treatment (Fig. 5A), and the antibody does not react with SAG1 under reducing conditions.

AT recognizes SAG1 and SAG3. To test whether the toxin-binding proteins of 32 and 38 kDa represented SAG1 and SAG3, respectively, we carried out toxin overlays on extracts of parasites deficient in these proteins (Fig. 6). The SAG1-deficient strain used in these studies was derived from the avirulent P(LK) strain. Direct comparison of Triton X-114 detergent-phase extracts from RH, P(LK), and P(LK)*sag1* tachyzoites confirmed that SAG1 is indeed a toxin-binding protein (Fig. 6A). The analysis also revealed a difference in the AT receptor profiles between the strains, in that relatively more toxin was bound to SAG1 from the P(LK) strain and to SAG3 from the RH strain (Fig. 6A). This result cannot be explained solely by differences in protein loads, because the corresponding silver-stained gel indicates that relatively more SAG1 was present in the detergent phase from RH (Fig. 6A). An additional AT-binding protein that migrates slightly above SAG1 was observed in P(LK) parasites; this protein was particularly evident in the SAG1-deficient parasites (Fig. 6A). A protein with similar electrophoretic mobility has been observed previously in this mutant (29). This analysis also revealed a potential mobility shift and/or shift in AT-binding specificity of the lower-molecular-mass proteins (~18 to 25 kDa) between the virulent and avirulent strains (Fig. 6A).

To test whether the 38-kDa toxin-binding protein was SAG3, we compared the toxin-binding profile of a SAG3-deficient mutant to that of its parental strain (Fig. 6B). The results clearly show that AT binds to SAG3. Both the AT overlay and the Western blots also show a subtle difference in the electrophoretic mobility of SAG3 from RH versus that from P(LK) parasites (Fig. 6A).

Aerolysin recognizes the same subset of receptors as AT. AT shares homology in structure and function to the large lobe of aerolysin, a pore-forming toxin from *Aeromonas hydrophila* (3, 14). Despite their similarities, AT and aerolysin exhibit differences in binding to specific mammalian GPI-anchored proteins (14, 15, 22). Aerolysin was found to kill *T. gondii* tachyzoites at concentrations similar to those of AT (data not shown). Furthermore, aerolysin recognized the same subset of parasite GPI-anchored proteins, including SAG3 and SAG1 (Fig. 6), and exhibited the same decrease in binding after PI-PLC treatment, which could again be abrogated by carrying out the electrophoresis under reducing conditions (data not shown). Aerolysin differed from AT in that SAG1 was the major aerolysin-binding protein from both RH and P(LK) strains (Fig. 6A). Aerolysin also recognized two additional proteins from the P(LK) strain, but not from the RH strain, which migrate slightly ahead of SAG3 (Fig. 6A, arrowheads); these bands may correspond to the SAG-related protein SRS2 (discussed below).

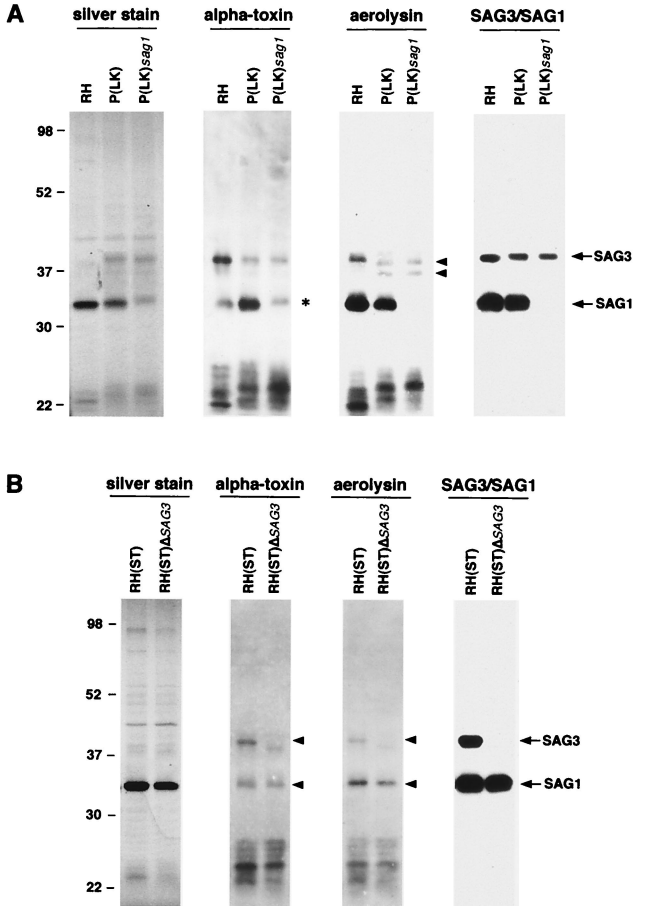

FIG. 6. (A) AT and aerolysin bind to SAG1. Triton X-114 detergent-phase fractions from RH, P(LK), and P(LK)*sag1* parasites were analyzed by SDS-PAGE followed by silver staining, AT overlay, aerolysin overlay, and immunoblotting with MAbs against SAG1 and SAG3. The SAG1 and SAG3 immunoblots were performed sequentially, and the data were combined digitally into the single panel shown. A 32-kDa toxin-binding band is observed in RH and P(LK) extracts that comigrates precisely with SAG1 on the corresponding immunoblot. Relatively more aerolysin binds to this protein [in both RH and P(LK) extracts] than does AT. SAG1-deficient parasites lack both immunoreactive SAG1 (as expected) and the 32-kDa toxin-binding protein. No other differences in the toxin-binding profiles were observed between P(LK) and the SAG1-deficient P(LK) parasites. Note that an additional 33-kDa AT-binding protein (asterisk) was observed in P(LK)*sag1* parasites that was not observed in RH parasites. The P(LK) and P(LK)*sag1* parasites also contained two aerolysin-binding bands not detected in RH parasites (arrowheads). Within each panel, equal amounts of protein were loaded per lane. Numbers on the left indicate molecular mass in kilodaltons. (B) AT and aerolysin bind to SAG3. Triton X-114 detergent-phase extracts from RH(ST) and SAG3-deficient RH(ST) parasites were analyzed as described above. A 38-kDa toxin-binding band is seen in RH(ST) extracts that comigrates precisely with SAG3 on the immunoblot. This 38-kDa toxin-binding band is absent in the RH(ST)Δ*SAG3* parasites, which, as expected, also lack immunoreactive SAG3. Numbers on the left indicate molecular mass in kilodaltons.

DISCUSSION

We have shown that *C. septicum* AT kills *T. gondii* tachyzoites in a potent and dose-dependent manner. The most conspicuous feature of AT-treated tachyzoites was the formation of a massive outward bleb in the parasite plasma membrane. Our data are consistent with a model in which AT binds to cell surface GPI-anchored proteins and inserts pores into the parasite plasma membrane. The resultant increase in osmotic pressure within the parasite leads to lysis of intracellular organelles and forces the cytoplasmic contents into the space between the IMC and plasma membrane. This ultimately leads to a localized disruption of the connection between the IMC and the plasma membrane and the formation of an outward bleb in the plasma membrane. The normally tight association between the plasma membrane and IMC was most evident in tachyzoites with ruptured blebs: these parasites exhibited an obvious gap in the plasma membrane, leaving the IMC exposed, while the remaining plasma membrane maintained a tight association with the IMC (Fig. 4B). Bridge-like structures, which may mediate the tight association between the plasma membrane and IMC, have been previously observed by electron microscopy (36), but the molecular nature of these structures remains unknown. The apparent stability of the IMC under osmotic stress may be due to the association of the IMC with the underlying tachyzoite cytoskeleton (reviewed in references 5 and 30).

The intracellular morphological effects of AT pore formation in nucleated cells have not been previously reported. In the case of aerolysin, pore formation in nucleated cells causes (in addition to lysis) plasma membrane ruffling and blebbing, followed by a microtubule-dependent fragmentation and vacuolation of the endoplasmic reticulum through an unknown mechanism (1). Our data from *T. gondii* provide the first direct evidence that, like aerolysin, AT is a vacuolating toxin. AT-treated tachyzoites often exhibited a large vacuole that appeared to be directly derived from the outer membrane of the nuclear envelope, a subcompartment of the tachyzoite endoplasmic reticulum (23). This result further demonstrates that the cellular consequences of pore formation by AT and aerolysin are conserved.

A requisite event for AT to exert these effects on a target cell is the binding of the toxin to GPI-anchored receptors on the cell surface and insertion of oligomerized toxin into the plasma membrane (4). The relative abundance of GPI-anchored proteins on the surface of protozoa is typically much higher than that of mammalian cells (31). For example, the GPI-anchored variant surface glycoprotein of *Trypanosoma brucei* is so densely packed that it restricts access of macromolecules to the underlying plasma membrane (48). The SAG proteins of *T. gondii* are also likely to be densely packed on the tachyzoite surface; SAG1 alone constitutes 3 to 5% of total tachyzoite protein (25), equivalent to approximately 1.5×10^6 to 2.5×10^6 molecules/cell. Nonetheless, AT ($\sim$ 44 kDa) can apparently both bind to GPI anchor targets and carry out the subsequent events necessary for pore formation on the tachyzoite plasma membrane.

Toxin overlays show that both AT and aerolysin recognize GPI-anchored proteins from *T. gondii* tachyzoites, including the major surface proteins SAG3 and SAG1 and multiple lower-molecular-mass ($\sim$18 to 25 kDa) proteins. Consistent with the presence of multiple AT-binding proteins on the surface of the parasite was the observation that wild-type and SAG3-deficient parasites exhibited no difference in AT sensi-

tivity by plaque assay (M.J.W. and G.E.W., unpublished observation).

The identities of the lower-molecular-mass toxin-binding proteins remain unknown. However, numerous tachyzoite SAG proteins have been identified with similar molecular masses, including SAG2A (19 kDa) (12, 28), SAG2B (23 kDa) (28), and an uncharacterized glycoprotein referred to as P23 (12, 33, 44), which migrates by SDS-PAGE as multiple species between 21 to 24 kDa (33). The pair of 35- and 37-kDa bands recognized uniquely by aerolysin in P(LK) strain parasites (Fig. 5A) may correspond to the SAG-related protein SRS2, which is more abundant in the P(LK) strain than RH and has previously been shown to migrate under nonreducing conditions as multiple species near SAG3 (29). The identity of the 54-kDa AT-binding protein that was recovered in the aqueous phase after Triton X-114 phase partitioning (Fig. 5A) is unknown.

The differential binding of AT to the individual *T. gondii* SAG proteins cannot be due solely to the relative abundance of these proteins, because SAG1 is by far the most abundant of the SAG proteins in RH strain parasites (27) (Fig. 5A, silver stain), yet it is not the major AT-binding protein. In contrast, SAG1 was the major toxin-binding protein from P(LK) parasites (Fig. 6A). The reasons for this difference between strains are unclear. The *SAG1* alleles from the RH and P(LK) strains diverge by eight amino acids, which could result in structural differences that may affect toxin binding in vitro (8, 9). SAG1 from RH is also predicted to have one potential N-linked glycosylation site, while SAG1 from P(LK) is predicted to have two. However, this site is not used in SAG1 from RH, and the sites in SAG1 from P(LK) are thought to be similarly unoccupied (6, 26, 33, 46). A third possibility would be differences in the structure of the GPI anchors of SAG1 between the two strains. The GPI anchor of SAG1 from RH parasites has been characterized, as have several glycolipid species that represent GPI anchor biosynthetic intermediates and a class of free GPIs (40–44, 49; Striepen et al., Biochem. Soc. Trans. **20:**296S, 1992; Tomavo et al., Biochem. Soc. Trans. **20:**166S, 1992). These studies indicate that GPI precursors and the mature GPI anchor of SAG1 contain the common trimannosyl core glycan found in most eucaryotic GPI anchors. Additionally, the SAG1 anchor is modified by addition of either a GalNAc or a GalNAc-glucose to the mannose proximal to the glucosamine residue, indicating that the mature GPI anchor of SAG1 from RH parasites has at least two possible glycoforms (49). The SAG1 GPI anchor from strains of *T. gondii* other than RH has not been characterized; however, our data suggest that subtle differences may indeed exist. Interestingly, the determinant(s) that differentially influences AT binding to SAG1 does not seem to similarly influence aerolysin binding, because SAG1 is the major aerolysin-binding protein from both strains.

The binding of AT and aerolysin to SAG proteins provides further evidence that the GPI anchor plays a crucial role in receptor recognition, because both toxins can bind to a variety of proteins from different organisms that are unrelated, except for the presence of a GPI anchor (13–15, 22). Consistent with studies on AT binding to mammalian GPI-anchored proteins (22), the glycosyl portion of the parasite GPI anchor harbors the AT binding determinant, because the toxin continued to recognize GPI-anchored proteins after PI-PLC delipidation. Removal of the lipid moiety resulted in a decrease in AT binding under nonreducing conditions; however, this decrease in toxin binding could be abrogated by reducing the samples prior to electrophoresis. The same phenomenon was observed with aerolysin (M.J.W. and G.E.W., unpublished observation). This suggests that delipidation may result in a conformational change in SAG proteins, which is consistent with the presence of conserved cysteine residues within the various members of the SAG family that are thought to contribute to the overall conformation of these proteins (9, 11, 27–29).

While GPI anchors represent the primary target for AT and aerolysin binding, it is less clear how specific GPI modifications, protein glycosylation (20, 24), or the contribution of the protein component itself influences this binding. *T. gondii* represents a unique experimental system for studying the molecular determinants that influence toxin binding, because the toxins exhibit preferential binding for certain SAG proteins within an individual strain and differences between strains. The binding studies have also revealed subtle differences in the electrophoretic mobility of several GPI-anchored proteins of RH and P(LK) strain parasites, the structural basis of which is unknown. Further studies on the differences between SAG proteins within and across different *T. gondii* strains may prove valuable for understanding the contributions of both protein and GPI anchor to receptor recognition by AT and aerolysin.

We have shown that *T. gondii* tachyzoites are susceptible to the cytolytic activity of AT at concentrations similar to those toxic to mammalian cells (22). AT represents a powerful new tool for the selection of a GPI-anchored protein deficiency in *T. gondii* and other susceptible protozoa in which databases and conventional molecular genetic approaches are limited. *T. gondii* is amenable to both chemical (35) and insertional (16) mutagenesis strategies, which we are currently pursuing to generate AT-resistant parasites.

ACKNOWLEDGMENTS

We thank J. Thomas Buckley for providing pro-aerolysin, Kim Carey for providing MAb 45.15; Doug Taatjes, Elaine Morbach, Jan Schwarz, and Marilyn Wadsworth for advice on electron microscopy; and Stanislas Tomavo for critical reading of the manuscript.

This work was supported by PHS grants AI42355 (G.E.W.), AI32097 (R.K.T.), and CA22435 (Vermont Cancer Center) and through the Vermont EPSCoR program under NSF grant EPS-9874685.

REFERENCES

1. **Abrami, L., M. Fivaz, P. E. Glauser, R. G. Parton, and F. G. van der Goot.** 1998. A pore-forming toxin interacts with a GPI-anchored protein and causes vacuolation of the endoplasmic reticulum. J. Cell Biol. **140:**525–540.
2. **Ballard, J., A. Bryant, D. Stevens, and R. K. Tweten.** 1992. Purification and characterization of the lethal toxin (alpha-toxin) of *Clostridium septicum*. Infect. Immun. **60:**784–790.
3. **Ballard, J., J. Crabtree, B. A. Roe, and R. K. Tweten.** 1995. The primary structure of *Clostridium septicum* alpha-toxin exhibits similarity with that of *Aeromonas hydrophila* aerolysin. Infect. Immun. **63:**340–344.
4. **Ballard, J., Y. Sokolov, W. L. Yuan, B. L. Kagan, and R. K. Tweten.** 1993. Activation and mechanism of *Clostridium septicum* alpha toxin. Mol. Microbiol. **10:**627–634.
5. **Black, M. W., and J. C. Boothroyd.** 2000. Lytic cycle of *Toxoplasma gondii*. Microbiol. Mol. Biol. Rev. **64:**607–623.
6. **Boothroyd, J. C., A. Hehl, L. J. Knoll, and I. D. Manger.** 1998. The surface of *Toxoplasma*: more and less. Int J. Parasitol. **28:**3–9.
7. **Bordier, C.** 1981. Phase separation of integral membrane proteins in Triton X-114 solution. J. Biol. Chem. **256:**1604–1607.
8. **Bulow, R., and J. C. Boothroyd.** 1991. Protection of mice from fatal *Toxoplasma gondii* infection by immunization with p30 antigen in liposomes. J. Immunol. **147:**3496–3500.
9. **Burg, J. L., D. Perelman, L. H. Kasper, P. L. Ware, and J. C. Boothroyd.** 1988. Molecular analysis of the gene encoding the major surface antigen of *Toxoplasma gondii*. J. Immunol. **141:**3584–3591.

10. **Carey, K. L., C. G. Donahue, and G. E. Ward.** 2000. Identification and molecular characterization of GRA8, a novel, proline-rich, dense granule protein of *Toxoplasma gondii*. Mol. Biochem. Parasitol. **105:**25–37.
11. **Cesbron-Delauw, M. F., S. Tomavo, P. Beauchamps, M. P. Fourmaux, D. Camus, A. Capron, and J. F. Dubremetz.** 1994. Similarities between the primary structures of two distinct major surface proteins of *Toxoplasma gondii*. J. Biol. Chem. **269:**16217–16222.
12. **Couvreur, G., A. Sadak, B. Fortier, and J. F. Dubremetz.** 1988. Surface antigens of *Toxoplasma gondii*. Parasitology **97:**1–10.
13. **Cowell, S., W. Aschauer, H. J. Gruber, K. L. Nelson, and J. T. Buckley.** 1997. The erythrocyte receptor for the channel-forming toxin aerolysin is a novel glycosylphosphatidylinositol-anchored protein. Mol. Microbiol. **25:**343–350.
14. **Diep, D. B., K. L. Nelson, T. S. Lawrence, B. R. Sellman, R. K. Tweten, and J. T. Buckley.** 1999. Expression and properties of an aerolysin-*Clostridium septicum* alpha toxin hybrid protein. Mol. Microbiol. **31:**785–794.
15. **Diep, D. B., K. L. Nelson, S. M. Raja, E. N. Pleshak, and J. T. Buckley.** 1998. Glycosylphosphatidylinositol anchors of membrane glycoproteins are binding determinants for the channel-forming toxin aerolysin. J. Biol. Chem. **273:**2355–2360.
16. **Donald, R. G., and D. S. Roos.** 1995. Insertional mutagenesis and marker rescue in a protozoan parasite: cloning of the uracil phosphoribosyltransferase locus from *Toxoplasma gondii*. Proc. Natl. Acad. Sci. USA **92:**5749–5753.
17. **Dzierszinski, F., M. Mortuaire, M. F. Cesbron-Delauw, and S. Tomavo.** 2000. Targeted disruption of the glycosylphosphatidylinositol-anchored surface antigen SAG3 gene in *Toxoplasma gondii* decreases host cell adhesion and drastically reduces virulence in mice. Mol. Microbiol. **37:**574–582.
18. **Ferguson, M. A.** 1999. The structure, biosynthesis and functions of glycosylphosphatidylinositol anchors, and the contributions of trypanosome research. J. Cell Sci. **112:**2799–2809.
19. **Ferguson, M. A., J. S. Brimacombe, S. Cottaz, R. A. Field, L. S. Guther, S. W. Homans, M. J. McConville, A. Mehlert, K. G. Milne, J. E. Ralton et al.** 1994. Glycosyl-phosphatidylinositol molecules of the parasite and the host. Parasitology **108:**S45–S54.
20. **Garland, W. J., and J. T. Buckley.** 1988. The cytolytic toxin aerolysin must aggregate to disrupt erythrocytes, and aggregation is stimulated by human glycophorin. Infect. Immun. **56:**1249–1253.
21. **Gordon, V. M., R. Benz, K. Fujii, S. H. Leppla, and R. K. Tweten.** 1997. *Clostridium septicum* alpha-toxin is proteolytically activated by furin. Infect. Immun. **65:**4130–4134.
22. **Gordon, V. M., K. L. Nelson, J. T. Buckley, V. L. Stevens, R. K. Tweten, P. C. Elwood, and S. H. Leppla.** 1999. *Clostridium septicum* alpha toxin uses glycosylphosphatidylinositol-anchored protein receptors. J. Biol. Chem. **274:**27274–27280.
23. **Hager, K. M., B. Striepen, L. G. Tilney, and D. S. Roos.** 1999. The nuclear envelope serves as an intermediary between the ER and Golgi complex in the intracellular parasite *Toxoplasma gondii*. J. Cell Sci. **112:**2631–2638.
24. **Howard, S. P., and J. T. Buckley.** 1982. Membrane glycoprotein receptor and hole-forming properties of a cytolytic protein toxin. Biochemistry **21:**1662–1667.
25. **Kasper, L. H.** 1987. Isolation and characterization of a monoclonal anti-P30 antibody resistant mutant of *Toxoplasma gondii*. Parasite Immunol. **9:**433–445.
26. **Kasper, L. H., M. S. Bradley, and E. R. Pfefferkorn.** 1984. Identification of stage-specific sporozoite antigens of *Toxoplasma gondii* by monoclonal antibodies. J. Immunol. **132:**443–449.
27. **Kasper, L. H., J. H. Crabb, and E. R. Pfefferkorn.** 1983. Purification of a major membrane protein of *Toxoplasma gondii* by immunoabsorption with a monoclonal antibody. J. Immunol. **130:**2407–2412.
28. **Lekutis, C., D. J. Ferguson, and J. C. Boothroyd.** 2000. *Toxoplasma gondii*: identification of a developmentally regulated family of genes related to SAG2. Exp. Parasitol. **96:**89–96.
29. **Manger, I. D., A. B. Hehl, and J. C. Boothroyd.** 1998. The surface of *Toxoplasma* tachyzoites is dominated by a family of glycosylphosphatidylinositol-anchored antigens related to SAG1. Infect. Immun. **66:**2237–2244.
30. **Mann, T., and C. Beckers.** 2001. Characterization of the subpellicular network, a filamentous membrane skeletal component in the parasite *Toxoplasma gondii*. Mol. Biochem. Parasitol. **115:**257–268.
31. **McConville, M. J., and M. A. Ferguson.** 1993. The structure, biosynthesis and function of glycosylated phosphatidylinositols in the parasitic protozoa and higher eukaryotes. Biochem. J. **294:**305–324.
32. **McConville, M. J., and A. K. Menon.** 2000. Recent developments in the cell biology and biochemistry of glycosylphosphatidylinositol lipids. Mol. Membr. Biol. **17:**1–16.
33. **Odenthal-Schnittler, M., S. Tomavo, D. Becker, J. F. Dubremetz, and R. T. Schwarz.** 1993. Evidence for N-linked glycosylation in *Toxoplasma gondii*. Biochem. J. **291:**713–721.
34. **Pfefferkorn, E. R., and S. E. Borotz.** 1994. *Toxoplasma gondii*: characterization of a mutant resistant to 6-thioxanthine. Exp. Parasitol. **79:**374–382.
35. **Pfefferkorn, E. R., and L. C. Pfefferkorn.** 1979. Quantitative studies of the mutagenesis of *Toxoplasma gondii*. J. Parasitol. **65:**364–370.
36. **Porchet-Hennere, E., and G. Nicolas.** 1983. Are rhoptries of coccidia really extrusomes? J. Ultrastruct. Res. **84:**194–203.
37. **Roos, D. S., R. G. Donald, N. S. Morrissette, and A. L. Moulton.** 1994. Molecular tools for genetic dissection of the protozoan parasite *Toxoplasma gondii*. Methods Cell Biol. **45:**27–63.
38. **Sellman, B. R., B. L. Kagan, and R. K. Tweten.** 1997. Generation of a membrane-bound, oligomerized pre-pore complex is necessary for pore formation by *Clostridium septicum* alpha toxin. Mol. Microbiol. **23:**551–558.
39. **Stevens, D. L., D. M. Musher, D. A. Watson, H. Eddy, R. J. Hamill, F. Gyorkey, H. Rosen, and J. Mader.** 1990. Spontaneous, nontraumatic gangrene due to *Clostridium septicum*. Rev. Infect. Dis. **12:**286–296.
40. **Striepen, B., J. F. Dubremetz, and R. T. Schwarz.** 1999. Glucosylation of glycosylphosphatidylinositol membrane anchors: identification of uridine diphosphate-glucose as the direct donor for side chain modification in *Toxoplasma gondii* using carbohydrate analogues. Biochemistry **38:**1478–1487.
41. **Striepen, B., C. F. Zinecker, J. B. Damm, P. A. Melgers, G. J. Gerwig, M. Koolen, J. F. Vliegenthart, J. F. Dubremetz, and R. T. Schwarz.** 1997. Molecular structure of the "low molecular weight antigen" of *Toxoplasma gondii*: a glucose alpha 1–4 *N*-acetylgalactosamine makes free glycosyl-phosphatidylinositols highly immunogenic. J. Mol. Biol. **266:**797–813.
42. **Tomavo, S., J. F. Dubremetz, and R. T. Schwarz.** 1992. Biosynthesis of glycolipid precursors for glycosylphosphatidylinositol membrane anchors in a *Toxoplasma gondii* cell-free system. J. Biol. Chem. **267:**21446–21458.
43. **Tomavo, S., J. F. Dubremetz, and R. T. Schwarz.** 1992. A family of glycolipids from *Toxoplasma gondii*. Identification of candidate glycolipid precursor(s) for *Toxoplasma gondii* glycosylphosphatidylinositol membrane anchors. J. Biol. Chem. **267:**11721–11728.
44. **Tomavo, S., J. F. Dubremetz, and R. T. Schwarz.** 1993. Structural analysis of glycosyl-phosphatidylinositol membrane anchor of the *Toxoplasma gondii* tachyzoite surface glycoprotein gp23. Biol. Cell **78:**155–162.
45. **Ward, G. E., and K. L. Carey.** 1999. 96-well plates providing high optical resolution for high-throughput, immunofluorescence-based screening of monoclonal antibodies against *Toxoplasma gondii*. J. Immunol. Methods **230:**11–18.
46. **Ware, P. L., and L. H. Kasper.** 1987. Strain-specific antigens of *Toxoplasma gondii*. Infect. Immun. **55:**778–783.
47. **Werk, R.** 1985. How does *Toxoplasma gondii* enter host cells? Rev. Infect. Dis. **7:**449–457.
48. **Ziegelbauer, K., and P. Overath.** 1993. Organization of two invariant surface glycoproteins in the surface coat of *Trypanosoma brucei*. Infect. Immun. **61:**4540–4545.
49. **Zinecker, C. F., B. Striepen, H. Geyer, R. Geyer, J. F. Dubremetz, and R. T. Schwarz.** 2001. Two glycoforms are present in the GPI-membrane anchor of the surface antigen 1 (P30) of *Toxoplasma gondii*. Mol. Biochem. Parasitol. **116:**127–135.

Editor: J. T. Barbieri